TiO_2 Hydrosols with Highly Photocatalytic Activity for Formaldehyde Degradation

Liu Tongxu[1, 4], Li Fangbai[2,*], Li Xiangzhong[3]

[1] *Guangzhou Institute of Geochemistry, Chinese Academy of Sciences, Guangzhou 510640, PR China*

[2] *Guangdong Key Laboratory of Agricultural Environment Pollution Integrated Control, Guangdong Institute of Eco-Environment and Soil Science, Guangzhou 510650, PR China*

[3] *Department of Civil and Structural Engineering, The Hong Kong Polytechnic University, Kowloon, Hong Kong, China*

[4] *Graduate School of the Chinese Academy of Sciences, Beijing 100039, PR China*

Abstract

Two kinds of TiO_2 hydrosols were prepared from titanium sulfate ($Ti(SO_4)_2$) and metatitanic acid (H_2TiO_3) by chemical precipitation-peptization method, and named as TSO and HTO, respectively. The as-obtained hydrosols were characterized by means of X-ray diffraction (XRD), particle size distribution (PSD), scanning electron microscopy (SEM), Brunauer – Emmett – Teller (BET) and Barret – Joyner - Halender (BJH) method, UV - Visible optical absorption spectra and transmittance spectra, and Fourier transform infrared spectra (FTIR). The results showed that TiO_2 hydrosols with anatase crystal structure had smaller particle sizes, higher surface areas and pore volume, and higher transparence, compared with P-25. In addition, TSO had an average size of 5.8 nm which was smaller than that of HTO (16.8 nm). The photocatalytic activity of TiO_2 hydrosols was evaluated for formaldehyde degradation under UVA light irradiation. The results showed that the photocatalytic activity for formaldehyde degradation was ranked as the order TSO > HTO > P-25. This investigation would be helpful to promote the industrialization and application of TiO_2 photocatalytic technique for indoor air purification.

Keywords: TiO_2 hydrosols; Formaldehyde; Photocatalytic activity; Indoor air purification

[*] *Corresponding author. Tel.:+86 20 87024721; Fax: +86 20 87024123. Email: cefbli@soil.gd.cn (F.B. Li).*

1. Introduction

Recently, indoor air quality (IAQ) within buildings has been paid great attention, since many metropolitan generally spend more than 80% of time in an indoor environment. The sick building syndrome has been a critical concern especially in some urban cities, such as Hong Kong, Guangzhou and Beijing, China [1,2]. Indoor air pollutants mainly include carbonyl compounds, nitrogen oxides (NO_x) and volatile organic compounds (VOCs), which can cause adverse health impacts on occupants [3]. These indoor air pollutants are emitted from different sources such as combustion byproducts, cooking, construction materials, office equipments, consumer products, and nearby traffic vehicles. Formaldehyde (HCHO) is a representative carbonyl compound, as one of the major indoor air pollutants, which comes from the furnishings and decorating materials, and frequently causes cancer and other sickness. In practice, the concentration of HCHO might usually be at ppbv to ppmv level in China [4-6]. Formaldehyde pollution has received much attention from people and government. In order to improve indoor air quality (IAQ), the abatement of formaldehyde has become the problem that should be urgently solved.

TiO_2 photocatalysis has become a very promising technique for the degradation of aqueous or gaseous toxic organic pollutants for water purification, wastewater treatment and air pollution control owing to its environmental benign [7-12]. TiO_2-based microsphere has been developed for the application for wastewater treatment because it can be used repeatedly [13-15]. At the meantime, TiO_2-based photocatalysts have also been paid enormous attention for its potential application for air pollution control owing to its higher photocatalytic activity [16-19], chemical stability and nontoxicity. However, it is not convenient to use TiO_2 powder to remove the air pollutions. Because it is very difficult to coat TiO_2 powder on wall, furnishings and decorating materials and it always changes their color. TiO_2 sol is a kind of convenient products because it is easy to obtain stable and firm TiO_2 thin film on coatings by means of spraying. The preparation of TiO_2 sols has been reported by means of hydrothermal process at low temperature. Some precursors including titanium butoxide ($Ti(OBu)_4$) [20], titanium ethoxide ($Ti(OC_2H_5)_4$) [21], titanium tetraisopropoxide ($Ti(OC_3H_7)_4$) [22], and titanium tetrachloride ($TiCl_4$) [23] were selected, while HNO_3, HCl, or tetraalkylammonium hydroxides (TANOHs) were selected as peptization catalysts. However, those TiO_2 sols contained a large amount of organic impurities when above-mentioned precursors or TANOHs were used. And if $TiCl_4$ was used as a precursor, the preparing condition was very strict due to its strong volatility. H_2TiO_3 and $Ti(SO_4)_2$,

as inorganic titanium sources with no volatility and lower costs, will be much worthy to apply in large scale production and application. In this study, two kinds of transparent TiO_2 hydrosols were prepared from $Ti(SO_4)_2$ or H_2TiO_3 by chemical precipitation-peptization method at low temperature (65^oC). The photocatalytic activity of TiO_2 hydrosols was evaluated for the degradation of formaldehyde under UVA illumination.

2. Experimental

2.1. Materials

Titanium sulfate ($Ti(SO_4)_2$) was analytical reagent grade from Shanghai Chemical Ltd. Metatitanic acid (H_2TiO_3) was from Panzhihua Iron & Steel Research Institute, China. Ammonium hydroxide (NH_4OH), nitric acid (HNO_3), and other chemicals were with analytical reagent quality and all obtained from Shanghai Reagent Ltd. The water with high purity was prepared by the RO system. Degussa P25 with 80% anatase and 20% rutile was obtained from Degussa AG Company in Germany.

2.2. Preparation of TiO_2 hydrosols

TiO_2 hydrosols were prepared by means of hydrothermal process, using $Ti(SO_4)_2$ and H_2TiO_3 as precursors. The process using $Ti(SO_4)_2$ was as follows: 120 g of $Ti(SO_4)_2$ was added into 2 L water, then transparent solution was obtained after stirring continuously for 1 hour. Then the ammonia was dropped therein very slowly until the pH value was above 9. The resulting suspension was stirred continuously for 3 hours, and then filtered. The filter cake was washed repeatedly for several times until no sulfate ion was present (determined by 0.5 mol/L barium chloride solutions) and pH value was near to neutral. In this way, the impurities could be substantively removed. Finally, the filter cake was mixed with deionized water to form uniform suspension. 200 ml of nitric acid with a concentration of 10% (v/v) was dropped therein to adjust the pH value to be between 1 and 2. The resulting suspension was stirred continuously for 4 hours at room temperature, followed by stirring and heating at a temperature of 65 ^oC. The suspension was peptized for 24 hours, and then titanium dioxide anatase hydrosol was obtained, named as TSO. The process by using metatitanic acid was as follows: 100 g of metatitanic acid was added into 2 L water, and then stirred continuously and uniform suspension is obtained. The other steps followed as the above process of TSO. The obtained TiO_2 hydrosol was named as HTO.

2.3. ***Characterization of TiO_2 hydrosols***

To characterize the properties by XRD, BET, SEM, and FTIR spectra, the titania xerogel powder was prepared through gelation treatment at 65 ^{o}C for 12 hours. The X-ray powder diffraction patterns were recorded on a Rigaku D/Max-III A diffract meter at room temperature, operating at 30 kV and 30 mA, using a Cu Kα radiation (λ = 0.15418 nm). The phases were identified by comparing diffraction patterns with those on the standard powder XRD cards compiled by the Joint Committee on Powder Diffraction Standards (JCPDS). The crystal sizes were calculated by Scherrer's formula [12,24]. If the sample contains anatase and brookite phases, the mass fraction of brookite can be calculated according to Eq. 1, where A_A and A_B represent the integrated intensities of the anatase (101) and brookite (121) peaks, respectively [24].

$$W_B = \frac{2.721A_B}{0.886A_A + 2.721A_B} \quad (1)$$

The specific surface area (S_{BET}) and total pore volume were measured by the Brunauer-Emmett-Teller (BET) method, in which the N_2 adsorption at 77 K was applied and an ASAP 2020 Sorptometer. The as-prepared xerogel sample was degassed at 90 ^{o}C prior to nitrogen adsorption measurements. Desorption isotherm was used to determine the pore size distribution by using the Barret-Joyner-Halender (BJH) method [25]. The nitrogen adsorption volume at the relative pressure (P/P_0) of 0.9733 was used to determine the pore volume and average pore sizes. The surface morphology of the catalysts was observed using scanning electron microscopy (SEM Leica Stereoscan 400i series). The particle size distributions (PSD) of the hydrosols were directly determined by a light-scattering size analyzer (Beckman N5, USA). The UV-visible absorption spectra and transmittance spectra in the wavelength range of 200-600 nm were obtained using a TU-1801 UV-visible spectrophotometer (Beijing, China). Fourier transform infrared spectra were recorded with a FTIR spectrometer (Perkin-Elmer) at room temperature.

2.4. The Photodegradation of formaldehyde

Formaldehyde was selected to evaluate the photocatalytic activity of the as-prepared TiO_2 hydrosols. The experiments of gaseous formaldehyde degradation were conducted at certain temperature (30±1 ^{o}C) and relative humidity (50±1%) using a 0.5 m^3 photoreactor made of stainless

steel. The reactor was placed in a small room where the temperature and humidity were well controlled. TiO_2 hydrosols or P-25 suspension were sprayed and coated onto four pieces of square glasses with a total area of about 1.0 m^2. The weight of catalysts for each experiment was kept at 1.00 g. The coated glasses were dried in an oven at 50 ^oC for about 2 hours to evaporate the adsorbed water and then cooled down to room temperature before used. The coated glasses were fixed in the reactor, and 8 sets of 15 W Philip UV lamps with the 365 nm peak were fixed above the coated glasses with 6 cm distance. The initial relative humidity before purging the formaldehyde was controlled by an air pump, which could blow dry or wet air. Then a certain amount of gaseous formaldehyde was purged into the photoreactor from the standard gaseous formaldehyde cylinder (Foshan, China). The formaldehyde was allowed to reach adsorption/ desorption equilibrium on the surface of catalyst in the reactor for 2 hours, prior to UV light irradiation. The initial concentration of formaldehyde after adsorption/desorption equilibrium was controlled at 5.5±0.2 ppmv, which remained constant for about 30 minutes until the UV lamps were turned on. The temperature and relative humidity were tested during photoreaction. The analysis of formaldehyde in the reactor was conducted with a formaldehyde monitor (Interscan 4160, USA). Each set of experiment lasted for 6 hours. On the basis of the experimental data, the plots of (C_t/C_0) versus t and the pseudo-first-order kinetic rate constants *k* were calculated.

3. Results and Discussion

3.1. XRD analyses

The crystal structure of TiO_2 hydrosol xerogel powders (TSO and HTO) was determined by means of X-ray diffraction (XRD), as shown in Fig. 1. The results showed that HTO should had pure anatase structure while TSO had dominant anatase structure and a weak brookite peak at 2θ=31° (about 5%). And the crystallinity of HTO was higher than that of TSO because the intensity of (101) peak for HTO was more than that of TSO. However, the crystallinity of P-25 was significantly higher than that of TSO and HTO, and P-25 powder had mixed crystal structure of anatase (about 80%) and rutile phase (about 20%). The crystal sizes of TSO and HTO estimated by the Scherrer equation were 5.57 nm and 11.3 nm, respectively, much less than that of P-25 (35.1 nm), as listed in Table 1. Generally, anatase TiO_2 powder with regular crystal structure could be obtained by sol-gel process and sintering at more than 400 ^oC. Hu and Yuan [26] reported anatase nanocrystalline particle could be obtained at 75 ^oC and

ambient pressure by hydrolysis of titanium-n-butoxide in abundant acidic solution, but it still had lots of organic compounds in the obtained sols. In this investigation, TiO_2 hydrosols with anatase structure were obtained at 65 ^oC and ambient pressure and they were organic-free due to the use of inorganic raw materials.

[Fig. 1.]

[Table 1]

3.2. Particle size distribution and morphology

The particle size distribution (PSD) is a very important property in deciding the stability and transparence of the hydrosols. As shown in Fig. 2, the PSD results demonstrated that HTO and TSO had a single-modal distribution characteristic with smaller particle sizes and more uniform PSD than P-25. The PSD of HTO was from 11.8 to 22.2 nm with the peak at 16.24 nm, and that of TSO was from 3.8 to 10.3 nm with the peak at 4.75 nm, while that of P-25 was 148 to 208 nm [27]. At the meantime, the average particle size was calculated on the basis of PSD analyses, as listed in Table 1. The results showed that TSO had an average size of 5.8 nm and HTO had an average size of 16.8 nm, while P-25 had an average size of 174 nm [27]. The particle sizes of TiO_2 sols by PSD were in good agreement with the crystal size by XRD. The average particle size of TSO (5.8 nm) was very close to its crystal size (5.57 nm), indicating an almost complete mono-dispersed hydrosol, while the average particle size of HTO (16.8 nm) was slightly more than its crystal size (11.3 nm), due to a slight aggregated hydrosol. Obviously, the average particle sizes of HTO and TSO were much less than that of titania sol (21 nm) prepared using titanium tetrachloride as precursor [28]. Additionally, it was clear that the average particle size of P-25 was much more than its crystal size, probably due to the severe aggregation during the calcinations process.

[Fig. 2.]

The morphology of TSO and HTO particles was examined by means of SEM, as shown in Fig. 3. Obviously, HTO particles were clear and the mixture of microporous and mesoporous structure formed was presented in Fig. 3(a). TSO particles and porous structure presented in Fig. 3(b) were not

very clear. From the XRD results, the anatase crystallinity of TSO was lower than that of HTO, indicating that more amorphous TiO_2 existed in TSO, which could be covered on the surface of crystalline TiO_2 particles.

[Fig. 3.]

3.3. BET surface areas and pore size distributions

To investigate the pore size distribution and adsorption properties of TiO_2 hydrosols, N_2 adsorption/desorption isothermal tests were carried out by means of BET-BJH method, and their isotherm curves were presented in Fig. 4(a). Both of isotherm curves for HTO and TSO showed Type IV curves. Their narrow hysteresis loops exhibited a typical pattern of Type II at a relative pressure from 0.4 to 0.6 (TSO) and 0.6 to 0.9 (HTO), indicating that these catalysts might have porous structures. The corresponding pore size distributions were shown in Fig. 4(b). Obviously, the pore size for TSO was dominantly distributed between 1.80 to 4.21 nm with the peak at 3.40 nm while that for HTO was dominantly distributed between 4 to 13 nm with the peak at 7.37 nm. The average pore size was calculated on the basis of pore size distribution data, and that of TSO was 2.8 nm, while that of HTO was 5.3 nm, as listed in Table 1. At the meantime, surface areas and average pore sizes were obtained by BET, as listed in Table 1. TSO had a significantly larger surface area of 379.0m^2/g, while HTO had also a large surface area of 286.8 m^2/g, which were much more than that of P-25 powders (63 m^2/g). Moreover, pore volume of HTO was 0.499cm^3/g while that of TSO was 0.200cm^3/g. It can be seen that a smaller particle size of TSO does not lead to a larger surface area than that of HTO. From the SEM results, the more amorphous TiO_2 existed in TSO may cover the pores and reduce the total surface areas.

[Fig. 4.]

3.4. UV-Vis transmittance spectra and absorption spectra

To determine the spectroscopic properties of TiO_2 hydrosols, the concentration of solid for TiO_2 hydrosols and P-25 were adjusted to the same concentration (0.050 wt %) in aqueous solution. The UV-visible transmittance spectra were shown in Fig. 5. Obviously, the transparence of TiO_2 hydrosols

and P-25 was ranked as the order TSO > HTO >>> P-25, which was in accordance with the order of particle sizes by PSD. A smaller particle size distribution leads to a better transparence.

[Fig. 5.]

The UV-visible absorption spectra were illustrated in Fig. 6. The results showed that both HTO and TSO did not show any optical absorption in visible region (wavelength more than 400 nm). The strong absorption in the ultraviolet range was attributable to the change-transfer process from 2p orbital of O^{2-} ions to t_{2g} orbital of the Ti^{4+} ions in the bulk TiO_2. Moreover, the optical absorption band-edge estimated at 348 nm for TSO and 368 nm for HTO obviously shifted to the blue direction compared with 387 nm for anatase TiO_2. Therefore, the particle size of hydrosols can affect significantly their optical properties. This blue shift has also agreement with the results by PSD, SEM and XRD.

[Fig. 6.]

3.5. FTIR analyses

Fig. 7 showed FTIR transmittance spectra (KBr pellets method) of TiO_2 hydrosol powders and P-25. The sharp bands at 1385 cm^{-1} are attributed to the coexisted NO_3^- groups from the peptization process because of the addition of HNO_3. And wide absorption bands at 400-750 cm^{-1} are corresponded to Ti-O for xerogel powders. The broad peaks at 3000-3500 cm^{-1} and the strong peak at 1634 cm^{-1} are attributed to O-H stretching vibration of water, Ti-OH group, and hydrated species on the TiO_2 surface. It showed that the surface hydroxyl groups of TSO and HTO were more than that of P-25, because the hydrosols were not treated at high temperature, and they avoided the severe aggregation among the thin particles.

[Fig. 7.]

3.6. Photocatalytic activity for formaldehyde degradation

In order to investigate the photocatalytic activity of anatase hydrosols, a set of gaseous experiments were carried out in a 0.5 m^3 photo-reactor at certain temperature (30±1 ^oC) and humidity (50±1%).

Formaldehyde was selected as pollutant for indoor air purification. The initial concentration of formaldehyde after adsorption/desorption equilibrium kept at a certain range of 5.5±0.2 ppmv. The photoreaction lasted for 6 hours. The degradation of gaseous formaldehyde under UV light illumination was shown in Fig. 8. Obviously, formaldehyde could be degraded effectively on the surface of TiO_2 catalysts. The removal percentage of formaldehyde was up to 88.9%, 82.4% and 62.0% for TSO, HTO, and P-25, respectively. The degradation of formaldehyde was well described by the pseudo-first-order kinetic. The pseudo-first-order kinetic constant (k) was shown in the inset of Fig. 8. The k value was 0.404, 0.326, and 0.181 h^{-1}, for TSO, HTO, and P-25, respectively. Obviously, the photocatalytic activity of TSO and HTO was significantly higher than that of P-25, and the k value of TSO was even 2.23 times of that of P-25.

[Fig. 8.]

The photoactivity for formaldehyde degradation (Fig. 8) were ranked as the order TSO > HTO > P-25, the same as that of particle sizes. Generally, the photocatalytic activity of TiO_2 should be a function of crystal structure, particle size, surface area and pore volume. Higher crystalline and smaller particle size should be beneficial to a higher photoactivity while a larger surface area and pore volume should lead to a higher adsorption capacity [24]. Under UV light irradiation, the dependence of the charge transfer on particle size might be decisive to photocatalytic reaction [7]. It had been reported that the charge carriers appeared to behave quantum mechanically when the particle size of a semiconductor particle fell below a critical radius of approximately 10 nm [8]. Compared with P-25, the TiO_2 hydrosols had lower anatase crystallinity, but they possessed smaller particle size, large surface area and pore volume (as listed in Table 1), which could enhance the efficiency of electron-hole separation and adsorption capacity, respectively. Additionally, despite of the highest BET surface area and pore volume, the photoactivity of HTO was significantly lower than that of TSO with the smallest particle size, indicating that particle size might play vital role in photoactivity for formaldehyde degradation.

4. Conclusion

TiO_2 hydrosols with highly photocatalytic activity for gaseous formaldehyde degradation were

prepared from titanium sulfate ($Ti(SO_4)_2$) and metatitanic acid (H_2TiO_3) by means of chemical precipitation-peptization method, respectively. The TiO_2 hydrosols had smaller particle sizes, narrower particle size distributions, larger surface areas and pore volumes, and better transparence, compared with P-25. The photoactivity for formaldehyde degradation were ranked as the order TSO > HTO > P-25. TSO with the smallest particle size (5.8 nm) had the highest activity for the photodegradation of formaldehyde. The synergic effects of smaller particle size and larger surface areas lead to the higher photocatalytic activity for the TiO_2 hydrosols, while the particle size played the most important role.

Acknowledgements

The authors are thankful to the National Natural Scientific Foundation of China (No.20203007 and 20377011) and Guangdong Innovative Technique Foundation (2005B10301001) for financial supports to this work.

References

[1] K. F. Ho, S. C. Lee, P. K. K. Louie, S. C. Zou, Seasonal variation of carbonyl compound concentrations in urban area of Hong Kong, Atmos. Environ. 36 (2002) 1259-1265.

[2] J. Zhang, W. Hu, F. Wei, G. Wu, L. Korn, R. S. Chapman, Children's respiratory morbidity prevalence in relation to air pollution in four Chinese cities, Environ. Heal. Persp. 100 (2002) 961-967.

[3] R. Atkinson, Atmospheric chemistry of VOCs and NOx, Atmos. Environ. 34 (2000) 2063-2101.

[4] Y. Feng, S. Wen, X. Wang, G. Sheng, Q. He, J. Tang and J. Fu, Indoor and outdoor carbonyl compounds in the hotel ballrooms in Guangzhou, China, Atmos. Environ. 38 (2004) 103-112.

[5] Z. Wang, Z. Bai, H. Yu, J. Zhang, T. Zhu, Regulatory standards related to building energy conservation and indoor-air-quality during rapid urbanization in China, Ener. Buil. 36 (2004) 1299-1308.

[6] Y. Zhao, B. Chen, Y. Guo, F. Peng, J. Zhao, Indoor air environment of residential buildings in Dalian, China, Ener. Buil. 36 (2004) 1235-1239.

[7] M. R. Hoffmann, S. T. Martin, W. Choi, B. W. Bahnemann, Environmental applications of semiconductor photocatalysis, Chem. Rev. 95 (1995) 69-96.

[8] P. V. Kamat, Photochemistry on nonreactive and reactive (semiconductor) surfaces, Chem. Rev. 93 (1993) 267-300.

[9] A. Fujishima, T.N. Rao, D. A.Tryk, Titanium dioxide photocatalysis, J. Photochem. Photobiol. C 1 (2001) 1-21.

[10] O. Carp, C. L. Huisman, A. Reller, Photoinduced reactivity of titanium dioxide, Prog. Solid State Chem. 32 (2004) 33-177.

[11] J. C. Yu, J. G. Yu, W. K. Ho, L. Z. Zhang, Preparation of highly photocatalytic active nano-sized TiO_2 particles via ultrasonic irradiation, Chem. Commun. (2001) 1942-1943.

[12] J. G. Yu, J. C. Yu, B. Cheng, S. K. Hark, K. Iu, The effect of F--doping and temperature on the structural and textural evolution of mesoporous TiO_2 powders, J. Solid State Chem. 174 (2003) 372-380.

[13] X. Z. Li, H. Liu, L. F. Cheng, H. J. Tong, Photocatalytic oxidation using a new catalyst - TiO_2 microsphere - for water and wastewater treatment, Environ. Sci. Technol. 37 (2003) 3989-3994.

[14] H. Liu, X. Z. Li, Y. J. Leng, W. Z. Li, An alternative approach to ascertain the rate-determining steps of TiO_2 photoelectrocatalytic reaction by electrochemical impedance spectroscopy, J. Phys. Chem. B 107 (2003) 8988-8996.

[15] H. Liu, H. T. Ma, X. Z. Li, and et al., The enhancement of TiO_2 photocatalytic activity by hydrogen thermal treatment, Chemosphere 50 (2003) 39-46.

[16] F. Shiraishi, S. Yamaguchi, Y. Ohbuchi, A rapid treatment of formaldehyde in a highly tight room using a photocatalytic reactor combined with a continuous adsorption and desorption apparatus, Chem. Eng. Sci. 58 (2003) 929-934.

[17] H. Liu, Z. Lian, X. Ye, W. Shangguan, Kinetic analysis of photocatalytic oxidation of gas-phase formaldehyde over titanium dioxid, Chemosphere 60 (2005) 630-635.

[18] P. Chin, L. P. Yang, D. F. Ollis, Formaldehyde removal from air via a rotating adsorbent combined with a photocatalyst reactor: Kinetic modeling, J. Catal. 237 (2006) 29-37.

[19] T. N. Obee, R. T. Brown, TiO_2 Photocatalysis for Indoor Air Applications: Effects of Humidity and Trace Contaminant Levels on the Oxidation Rates of Formaldehyde, Toluene, and 1, 3-Butadiene, Environ. Sci. Technol. 29 (1995) 1223-1231.

[20] J. Yang, S. Mei, J. M. F. Ferreira, In situ preparation of weakly flocculated aqueous anatase suspensions by a hydrothermal technique, J. Colloid Interf. Sci. 260 (2003) 82-88.

[21] J. Yang, S. Mei, J. M. F. Ferreira, Hydrothermal synthesis of TiO_2 nanopowders from tetraalkylammonium hydroxide peptized sols, Mater. Sci. Eng. C 15 (2001) 183-185.

[22] F. Cot, A. Larbot, G. Nabias, L. Cot, Preparation and characterization of colloidal solution derived crystallized titania powder, J. Euro. Ceram. Soc. 18 (1998) 2175-2181.

[23] D. Lee, T. Liu, Preparation of TiO_2 Sol Using $TiCl_4$ as a Precursor, J. Sol-Gel Sci. Technol. 25 (2002) 121-136.

[24] J. G. Yu, M. H. Zhou, B. Cheng, H. G. Yu, X. J. Zhao, Ultrasonic preparation of mesoporous titanium dioxide nanocrystalline photocatalysts and evaluation of photocatalytic activity, J. Mol. Catal. A 227 (2005) 75-80.

[25] S. L. Gregg, K. S. W. Sing, Adsorption, Surface Area and Porosity, Academic Press, London, 1982.

[26] Y. Hu, C. Yuan, Low-temperature preparation of photocatalytic TiO_2 thin films from anatase sols, J. Cryst. Growth. 274 (2005) 563-568.

[27] Y. B. Xie, C. W. Yuan, Visible-light responsive cerium ion modified titania sol and nanocrystallites for X-3B dye photodegradation, Appl. Catal. B 46 (2003) 251-259.

[28] Y. B. Xie, C. W. Yuan, X. Z. Li, Photocatalytic degradation of X-3B dye by visible light using lanthanide ion modified titanium dioxide hydrosol system, Colloids Surf. A 252 (2004) 87-94.

Figure captions

Fig. 1. X-ray diffraction patterns (XRD) of P-25 powder, the sol particles of HTO and TSO.

Fig. 2. Particle size distributions (PSD) of TSO and HTO.

Fig. 3. Scanning electron microscopy (SEM) of the sol particles of HTO (a) and TSO (b).

Fig. 4. N_2 adsorption-desorption isotherms of the sol particles of HTO and TSO (a); pore size distributions of the sol particles of TSO and HTO (b).

Fig. 5. UV-Visible transmittance spectra of TSO, HTO and P-25 suspension.

Fig. 6. UV-Visible absorbance spectra of TSO and HTO**.**

Fig. 7. FTIR transmittance spectrum of the TiO_2 sol particles of HTO and TSO.

Fig. 8. Photocatalytic activity and the pseudo-first-order kinetic constants (h^{-1}) of HTO, TSO and P-25 suspension for the degradation of formaldehyde.

Table 1

The crystal structure, crystal size, particle size, surface area, pore volume, pore size of HTO, TSO and P-25 powder

Sample	[a] Crystal structure	[b] Crystal size (nm)	[c] Particle size (nm)	[d] Surface area (m^2/g)	[e] Pore volume (cm^3 /g)	[e] Pore size (nm)
HTO	A	11.3	16.8	379.0	0.499	5.3
TSO	A +B (5%)	5.57	5.8	286.8	0.200	2.8
P-25[27]	A+R (20%)	35.1	174	63.0	0.060	/

[a] A, B and R denote anatase, brookite and rutile, respectively. [b] Crystal size of TiO_2 was determined by XRD using Scherrer equation. [c] Average particle size was determined by PSD. [d] The BET surface area was determined by multipoint BET method using the adsorption data. [e] Pore volume and average pore size were determined by nitrogen adsorption at the relative pressure (P/P_0) of 0.9733.

Fig. 1.

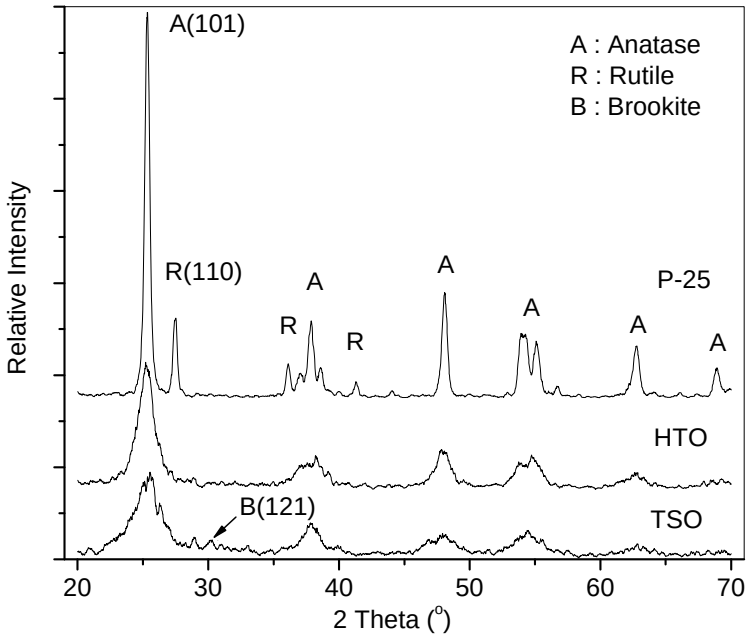
A(101)
A : Anatase
R : Rutile
B : Brookite
R(110)
A
R
R
A
A
A
A
P-25
HTO
B(121)
TSO
Relative Intensity
20
30
40
50
60
70
2 Theta (°)

Fig. 2.

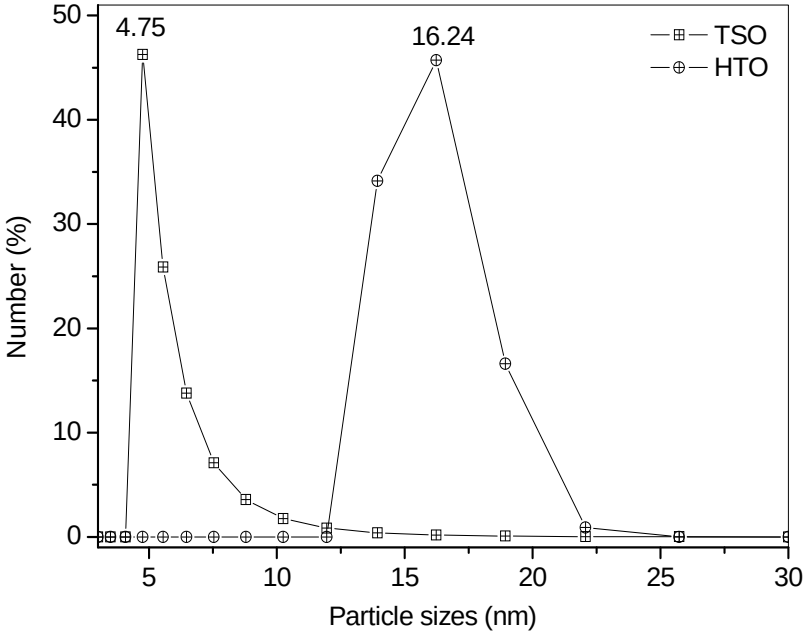
4.75
16.24
TSO
HTO
Number (%)
Particle sizes (nm)
0
10
20
30
40
50
5
10
15
20
25
30

Fig. 3.

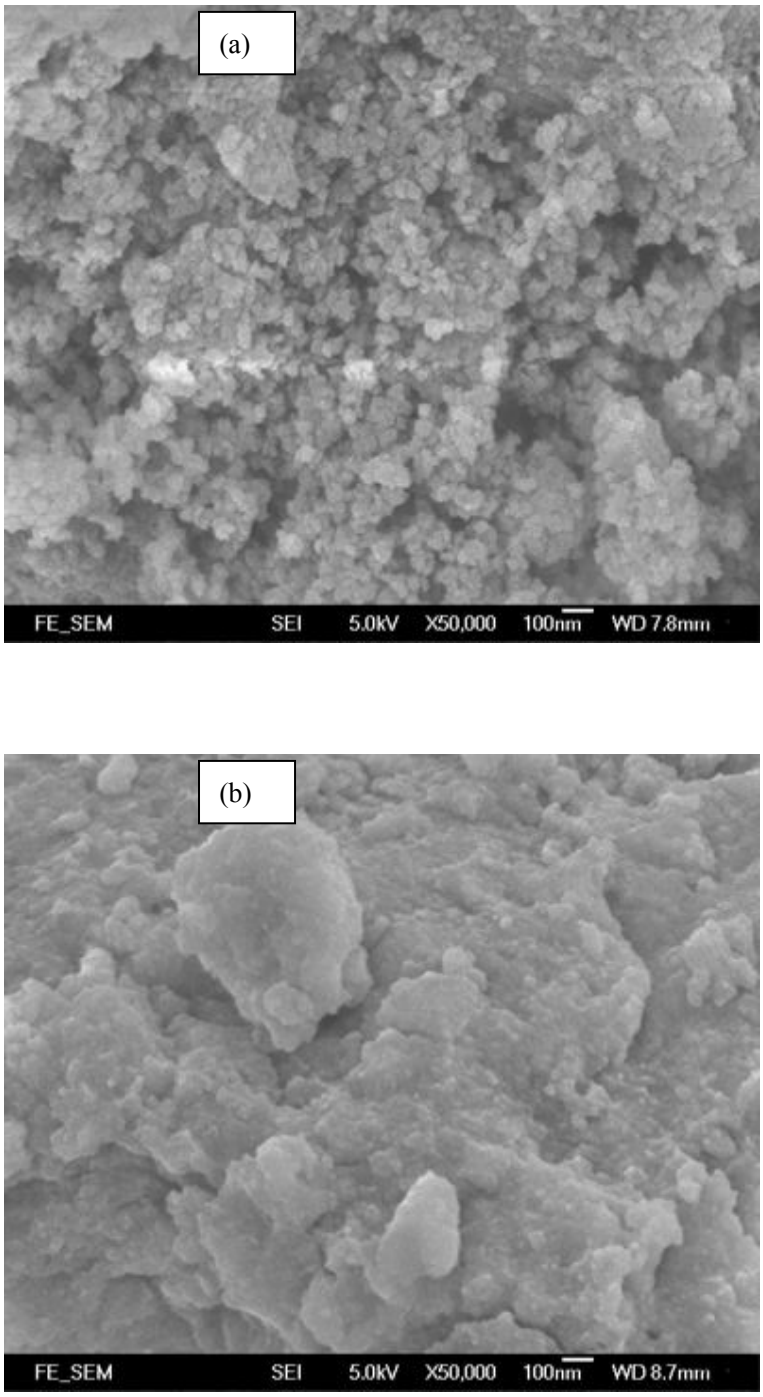
(a)
FE_SEM SEI 5.0kV X50,000 100nm WD 7.8mm
(b)
FE_SEM SEI 5.0kV X50,000 100nm WD 8.7mm

Fig. 4.

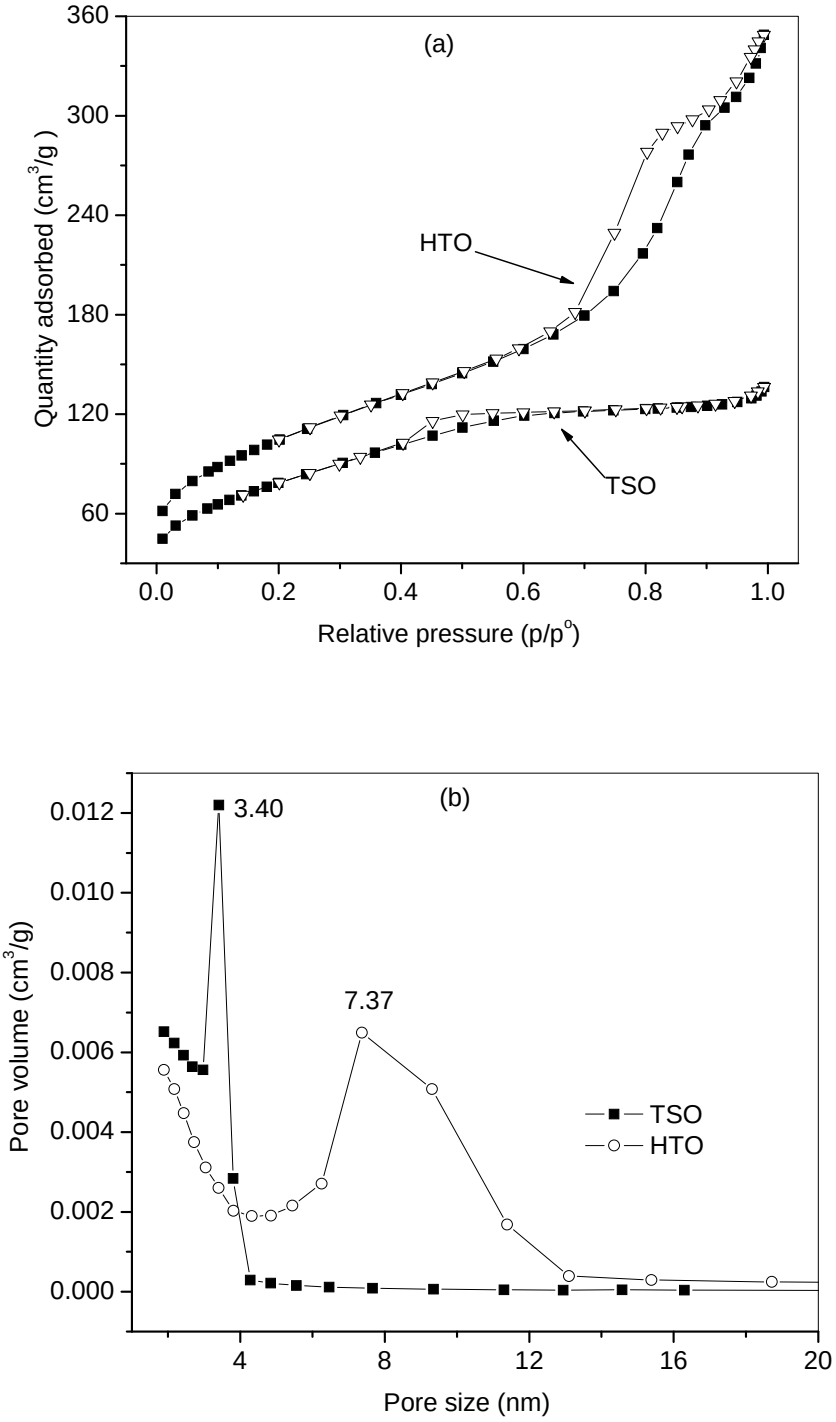
(a)
Quantity adsorbed (cm3/g)
Relative pressure (p/po)
HTO
TSO
360
300
240
180
120
60
0.0
0.2
0.4
0.6
0.8
1.0
(b)
Pore volume (cm3/g)
Pore size (nm)
3.40
7.37
TSO
HTO
0.012
0.010
0.008
0.006
0.004
0.002
0.000
4
8
12
16
20

Fig. 5.

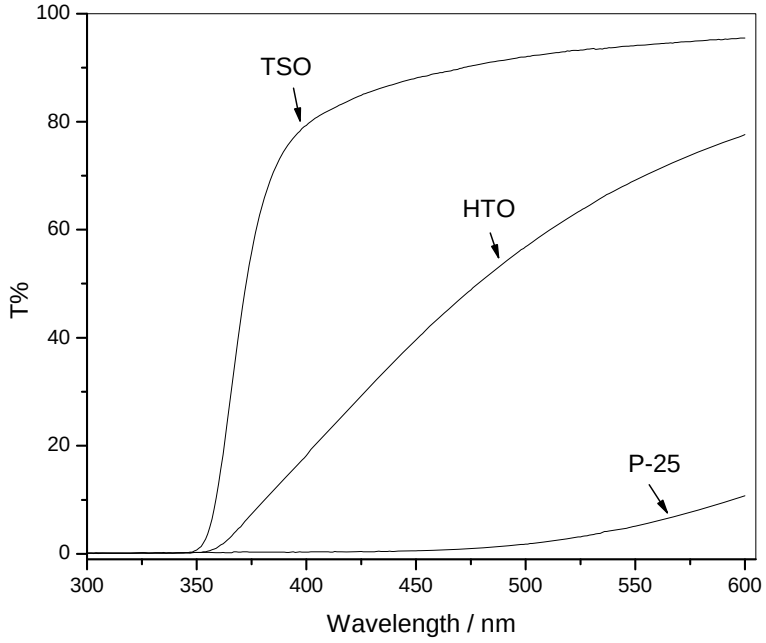
100
80
60
40
20
0
T%
TSO
HTO
P-25
300
350
400
450
500
550
600
Wavelength / nm

Fig. 6.

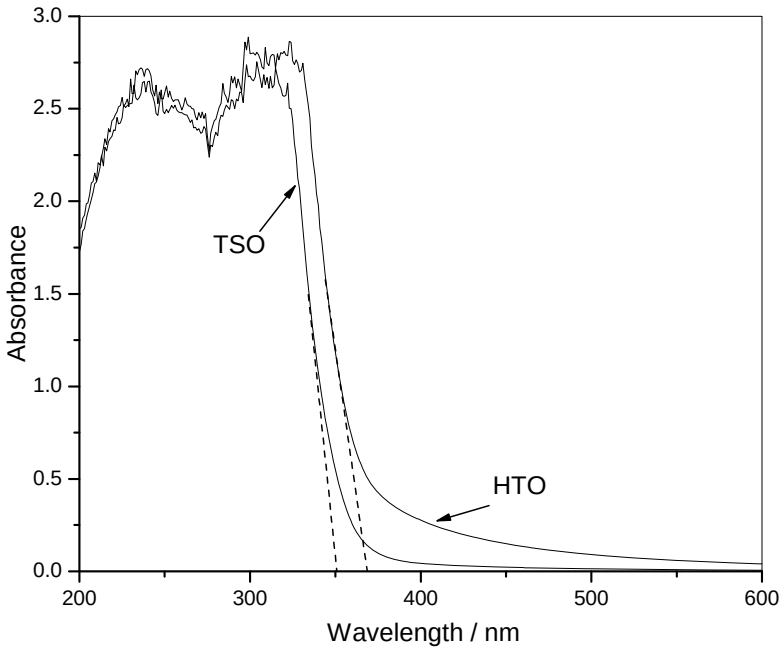
3.0
2.5
2.0
1.5
1.0
0.5
0.0
Absorbance
200
300
400
500
600
Wavelength / nm
TSO
HTO

Fig. 7.

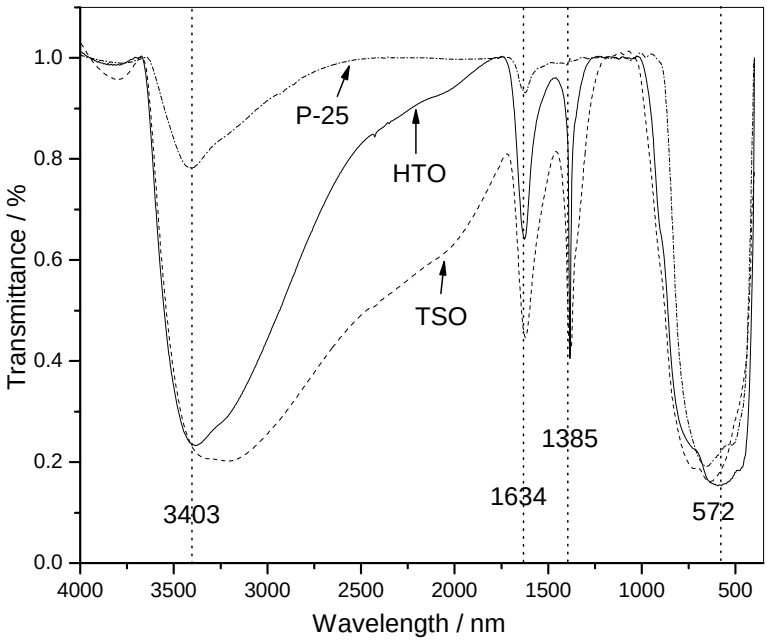
Transmittance / %
Wavelength / nm
P-25
HTO
TSO
3403
1634
1385
572
1.0
0.8
0.6
0.4
0.2
0.0
4000
3500
3000
2500
2000
1500
1000
500

Fig. 8.

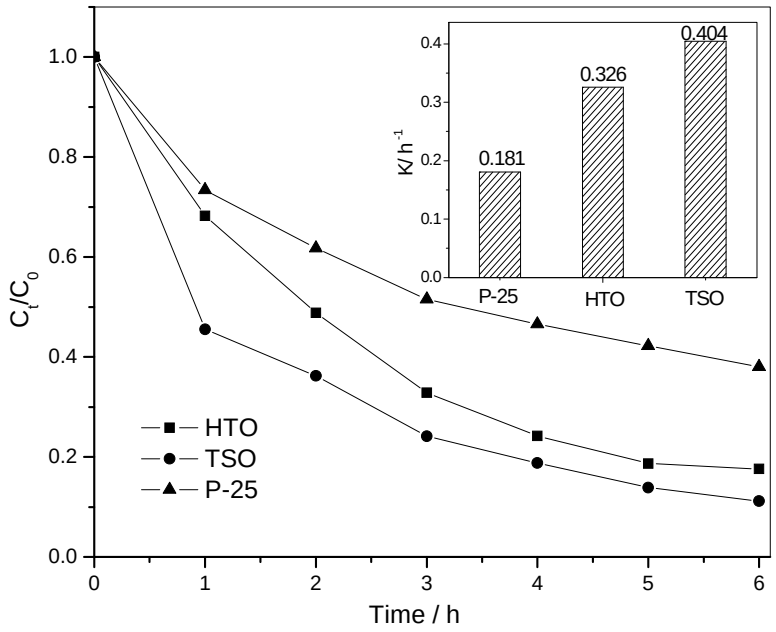
1.0
0.8
0.6
0.4
0.2
0.0
C_t/C_0
0
1
2
3
4
5
6
Time / h
HTO
TSO
P-25
0.4
0.3
0.2
0.1
0.0
K/ h^{-1}
0.181
0.326
0.404
P-25
HTO
TSO